ELSEVIER

Journal of Power Sources 114 (2003) 63–69

JOURNAL OF POWER SOURCES

www.elsevier.com/locate/jpowsour

The performance of PEM fuel cells fed with oxygen through the free-convection mode

Pei-Wen Li*, Tao Zhang, Qing-Ming Wang, Laura Schaefer, Minking K. Chyu

Department of Mechanical Engineering, Benedum Engineering Hall, University of Pittsburgh, Pittsburgh, PA 15261, USA

Received 17 September 2002; accepted 27 September 2002

Abstract

The feasibility and restrictions of feeding oxygen to a PEM fuel cell through free-convection mass transfer were studied through theoretical analysis and experimental testing. It was understood through the theoretical analysis that the free-convection mass-transfer coefficient strongly depends on the difference in mass fraction or concentration of oxygen at the cathode surface and in the quiescent air. Thus, the mass-transfer rate has a strong dependence on the oxygen concentration at the cathode surface, which can be viewed in terms of the relationship of the fuel cell current density and the fuel cell voltage. Through this analysis, the maximum applicable current density was derived, beyond which there will be an abrupt drop in the output voltage, which results in excessively low power in the fuel cell. Experimental tests were conducted for one PEM fuel cell stack and two single PEM fuel cell units. An excessive drop in output voltage was observed when the free-convection mass-transfer mode was utilized. It was also found that the orientation of the cathode surface affects the performance of the fuel cell, which is mainly due to the fact that the free-convection mass-transfer coefficient depends on the orientation of the involved mass-transfer surface, which is analogous to free-convection heat transfer.

Keywords: Free-convection mass transfer; PEM fuel cell; Theoretical analysis; Experimental test

1. Introduction

A fuel cell is a device which converts chemical energy from a chemical reaction directly into electrical energy, and thus has a high energy conversion efficiency compared to devices based on thermal–mechanical–electrical energy conversion processes [1,2]. The low emission of pollutants and high electrical conversion efficiency make this technology attractive, and it is currently being considered as the most promising candidate for a variety of scales of power sources, from portable devices to stationary and automotive applications. There is no doubt that fuel cells might eventually supplant traditional power systems (batteries, thermoelectric power plants and internal combustion engines) [3,4].

A fuel cell must be continually fed with fuel (hydrogen, methanol, etc.) and oxidant (oxygen). Since it is easy to get, air is used in most situations to provide oxygen to a fuel cell [5,6]. Although a fan or blower could be used to feed air to a fuel cell, each consumes a certain amount of power and may most probably be adopted for large-scale fuel cells and fuel cell stacks. For small power fuel cells or where pumping or a fan system is not available, the present authors propose that natural convection mass transfer be utilized for the fuel cell to obtain oxygen from the air. There is no doubt that free-convection has a smaller mass-transfer coefficient and thus restricts the maximum available current density of the fuel cell. This is analyzed and reviewed in the paper, and an experimental investigation for a miniaturized fuel cell is conducted which relies on natural convection mass transfer for its oxidant/oxygen.

From the point of view of free-convection heat transfer, the orientation of the heat-transfer surface might affect the heat-transfer coefficient [7,8]. Analogous to free-convection heat transfer, free-convection mass transfer will have similar characteristics. This will also be investigated through both theoretical analysis and experimental testing.

2. Analysis of free-convection mass transfer

2.1. Analogy of free-convection heat and mass transfer

Free-convection mass transfer will have common characteristics with free-convection heat transfer, the latter having been studied extensively, if they share analogous

* Corresponding author. Tel.: +1-412-624-9798; fax: +1-412-624-4846.
E-mail address: pel1@pitt.edu (P.-W. Li).

0378-7753/02/$ – see front matter
PII: S0378-7753(02)00535-9

Nomenclature

D	mass diffusion coefficient (m^2/s)
E	electromotive force (EMF) of fuel cell (V)
f	represent a function
F	Faraday's constant (96496.7 C/mol)
g	gravitational acceleration (9.807 m/s^2)
ΔG_0	standard state Gibb's free energy change for water, formed from oxygen and hydrogen
Gr	Grashof number
h	mass-transfer coefficient (m/s)
i	current density of fuel cell (mA/cm^2)
L	characteristic length (m)
m	mass flux ($kg/(m^2\ s)$)
M	formula weight (g/mol)
Nu	Nusselt number
P	pressure (Pa)
Pr	Prandtl number
R	universal gas constant (8.314 J/(mol K))
Ra	Rayleigh number
Sc	Schmidt number
Sh	Sherwood number
T	temperature (K)
w	mass fraction (0–1.0)

Greek symbols

γ	expansion coefficient due to mass fraction gradient
v	kinematic viscosity (m^2/s)
ρ	density (kg/m^3)

Superscripts

H_2O	water vapor
O_2	oxygen

Subscripts

1	gas number 1 of a two-gas mixture
air	air
H_2	hydrogen
H_2O	water vapor
L	based on characteristic length L
M	mass transfer
N_2	nitrogen
O_2	oxygen
P	at pressure P
w	at surface or wall
∞	in quiescent air

boundary conditions and the same geometry [7]. In studies of free-convection heat transfer, the heat-transfer coefficient can be obtained from empirical equations in terms of the Nusselt number as a function of the Grashof number or Rayleigh number as well as the Prandtl number [8]:

$$Nu = f(Ra, Pr) \tag{1}$$

On the other hand, it is known that the analogy between the boundary-layer equations describing heat transfer and equations for isothermal mass transfer can lead to the conclusion that there exists for every heat-transfer situation a corresponding mass-transfer situation with analogous boundary conditions and the same geometry. For such an analogous mass transfer, by simply replacing Nusselt number in the corresponding relation for heat transfer by the Sherwood number, the Rayleigh number, Ra, by the Rayleigh number, Ra_M, for mass transfer, and the Prandtl number, Pr, by the Schmidt number, Sc, the following can be obtained:

$$Sh = f(Ra_M, Sc) \tag{2}$$

In an analogous derivation, one can obtain the Grashof number:

$$Gr_M = \frac{\gamma g(w_{1w} - w_{1\infty})L^3}{v^2} \tag{3}$$

or the Rayleigh number:

$$Ra_M = Gr_M Sc = \frac{\gamma g(w_{1w} - w_{1\infty})L^3}{vD} \tag{4}$$

for mass transfer.

As with the expansion coefficient in free-convection heat transfer, the mass-transfer free-convection effects depend on the expansion coefficient, γ:

$$-\frac{1}{\rho}\left(\frac{\partial \rho}{\partial w_1}\right)_P = \gamma \tag{5}$$

The manner in which γ is obtained depends on the gas mixture. For mass transfer between two ideal gases, it can be further expressed, through derivation, as

$$-\frac{1}{\rho}\left(\frac{\partial \rho}{\partial w_1}\right)_P = \frac{M_2 - M_1}{(w_1 M_2) + ((1 - w_1)M_1)} \tag{6}$$

While there are rarely equations specifically for the free-convection mass-transfer coefficient, some well-known empirical equations of the free-convection heat-transfer coefficient can be utilized based on the above discussion.

A few useful equations for free-convection heat-transfer coefficient are further outlined here. For the heat transfer of a plate with the orientation that the heated surface is horizontally upward [8]:

$$\overline{Nu}_L = 0.54 Ra_L^{1/4} \quad (10^4 \le Ra_L \le 10^7) \tag{7}$$

$$\overline{Nu}_L = 1.5 Ra_L^{1/3} \quad (10^7 \le Ra_L \le 10^{11}) \tag{8}$$

If the heated surface is horizontally downward:

$$\overline{Nu}_L = 0.27 Ra_L^{1/4} \quad (10^5 \le Ra_L \le 10^{10}) \tag{9}$$

When the heated surface of the plate is oriented vertically, the applicable equation for the heat-transfer coefficient is

$$\overline{Nu}_L = 0.68 + \frac{0.67 Ra_L^{1/4}}{[1 + (0.492/Pr)^{9/16}]^{4/9}} \quad (Ra_L \le 10^9) \tag{10}$$

Turning to the mass-transfer problem, we can derive the following analogous equations:

$$\overline{Sh}_L = 0.54 Ra_M^{1/4} \quad (10^4 \le Ra_M \le 10^7) \tag{11}$$

$$\overline{Sh}_L = 0.15 Ra_M^{1/3} \quad (10^7 \le Ra_M \le 10^{11}) \tag{12}$$

for the case that reaction surface is oriented upward. And when the reaction surface is downward:

$$\overline{Sh}_L = 0.27 Ra_M^{1/4} \quad (10^5 \le Ra_M \le 10^{10}) \tag{13}$$

In case the reaction surface is oriented vertically, we have:

$$\overline{Sh}_L = 0.68 + \frac{0.67 Ra_M^{1/4}}{[1 + (0.492/Sc)^{9/16}]^{4/9}} \quad (Ra_M \le 10^9) \tag{14}$$

Even though the precision of these mass-transfer equations may be subject to some uncertainty, they are, however, very useful for qualitative analysis.

2.2. Applicable fuel cell current density due to the restriction of free-convection mass transfer

Considering the free convective diffusion of oxygen from ambient quiescent air to the electrochemical reaction site of the cathode surface, the available mass flux at the cathode surface can be expressed as

$$m_{O_2} = h_M^{O_2} \rho_{air} (w_\infty^{O_2} - w_w^{O_2}) \tag{15}$$

The mass fraction of oxygen in the ambient air is approximately 0.21 [9]. From knowledge of the electrochemical reaction of a PEM fuel cell [10–12], the correlation between the current density and the mass flux of oxygen is

$$i = \frac{m_{O_2}}{M_{O_2}} (4F) \tag{16}$$

Given a series of current densities, one can find the corresponding mass fractions or concentrations of oxygen at the cathode surface. This mass fraction at the cathode surface has to be restricted between 0 and 0.21 for oxygen, which conversely is a condition to restrict the maximum mass flux of oxygen or the maximum potential current density of the fuel cell.

Here we consider a cathode surface having a characteristic length of $L = 0.08$ m (to allow for a Ra_M large enough and applicable for Eqs. (11)–(14)) and exposed to ambient quiescent air in three orientations, downward, upward, and vertically under the conditions of 25 °C and 1 atm. When the diffusion of oxygen is considered, we neglect the existence of water vapor at the PEM fuel cell cathode surface. Then the diffusion of oxygen in nitrogen can be treated using the method outlined above. Simply from a mass-transfer point of view, Fig. 1 gives the applicable current density of a fuel cell against the surface oxygen mass fraction based on free-convection mass transfer. A monotonic decrease of the oxygen mass fraction can be seen in the figure. Due to the different orientations of the reaction surface and the correspondingly different mass-transfer coefficients, the available current density shows some differences. It is clear, however, that the available current density may increase with an increasing mass-transfer coefficient. This indicates that a higher mass fraction or concentration of oxygen on the cathode surface may be maintained if one selects a better orientation of the surface for obtaining a higher mass-transfer coefficient.

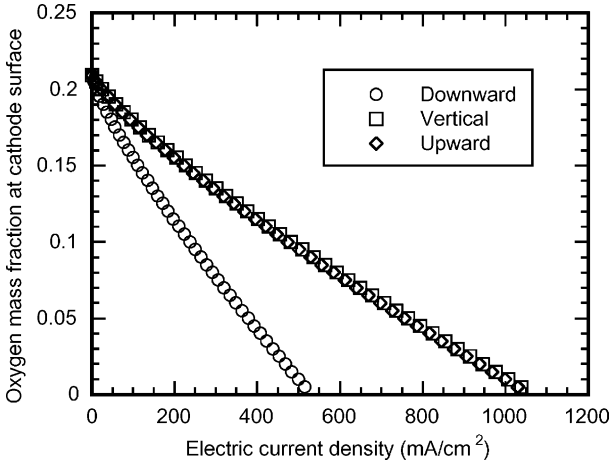

Fig. 1. Current density vs. mass fraction of oxygen at the cathode surface based on free-convection mass transfer.

The mass fraction of oxygen at the cathode surface will influence the fuel cell voltage, which can be seen from the Nernst equation:

$$E = \frac{-\Delta G_0}{2F} + \frac{RT}{2F} \ln\left(\frac{P_{H_2} P_{O_2}^{0.5}}{P_{H_2O}}\right) \tag{17}$$

The partial-pressure of oxygen in the equation can be expressed in terms of the mass fraction of the oxygen:

$$P_{O_2} = \frac{w_w^{O_2}/M_{O_2}}{(w_w^{O_2}/M_{O_2}) + ((1 - w_w^{O_2})/M_{N_2})} P \tag{18}$$

In order to see the influence of the oxygen mass fraction on the fuel cell electromotive force from the curves in Fig. 1, the oxygen partial-pressure-related term, $\ln(P_{O_2}^{0.5})$, in Eq. (17) is plotted versus the current density in Fig. 2. An excessive drop of $\ln(P_{O_2}^{0.5})$ can be found when the current density is beyond a certain extent; for example, 300 mA/cm^2 for the downward orientation. The contribution of the term $\ln(P_{O_2}^{0.5})$ to the electromotive force, E, is positive. Therefore, an excessive drop of $\ln(P_{O_2}^{0.5})$ could result in an excessive drop of the electromotive force, E.

In a similar manner, when considering the free-convection mass transfer of water vapor at the cathode surface, the existence of oxygen is neglected. Therefore, for the two gases' diffusion of nitrogen and water vapor, there are similar equations to find the relationship between the fuel

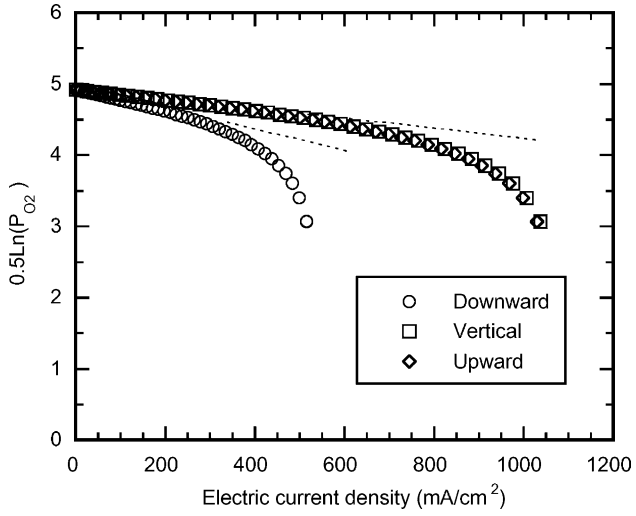

Fig. 2. Relationship of the current density and the logarithm of the oxygen partial-pressure at the cathode surface.

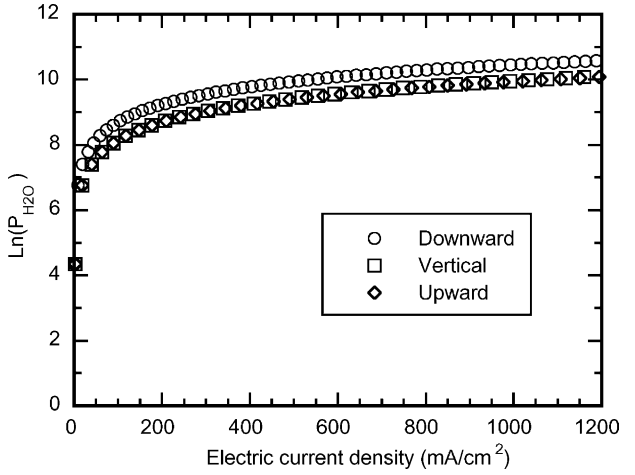

Fig. 4. Relationship of the current density and the logarithm of partial-pressure for water vapor at the cathode surface.

cell current density and the mass fraction of water vapor at the cathode surface:

$$m_{H_2O} = h_M^{H_2O} \rho_{air} (w_w^{H_2O} - w_\infty^{H_2O}) \quad (19)$$

$$i = \frac{m_{H_2O}}{M_{H_2O}} (2F) \quad (20)$$

$$P_{H_2O} = \frac{w_w^{H_2O}/M_{H_2O}}{(w_w^{H_2O}/M_{H_2O}) + ((1 - w_w^{H_2O})/M_{N_2})} P \quad (21)$$

Suppose the mass fraction of water vapor in the quiescent ambient air is zero. The mass fractions of water vapor at the cathode surface could be derived via a series of current densities of a PEM fuel cell. Fig. 3 shows that the water vapor mass fraction increases with an increase in current density. Corresponding to the higher mass-transfer coefficient, the mass fraction of water vapor at the cathode surface is relatively low under the same current density.

Using Eq. (21), the logarithm of the partial-pressure of water vapor, $\ln(P_{H_2O})$, can be deduced as function of the fuel cell current density based on the curves in Fig. 3. Fig. 4 shows that $\ln(P_{H_2O})$ increases with the fuel cell current density. Due to the different values of the mass-transfer coefficients under the different orientations of the mass-transfer surfaces, the value of $\ln(P_{H_2O})$ shows some variation. For the case of a downward oriented mass-transfer surface, which corresponds to a lower mass-transfer coefficient, the $\ln(P_{H_2O})$ is higher under the same fuel cell current density.

Shown in Fig. 5 is the difference between the logarithm partial-pressure terms of oxygen and water vapor, which reflects how the free-convection mass transfer at the cathode surface affects the cell voltage. Because the value of $(\ln(P_{O_2}^{0.5}) - \ln(P_{H_2O}))$ partly reflects the variation of the fuel cell electromotive force, it shows a very similar style to the

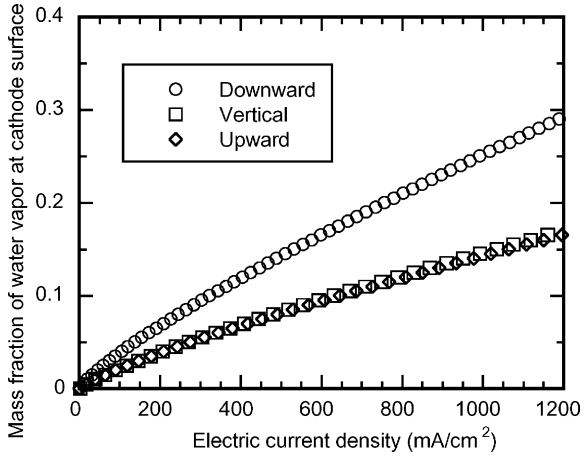

Fig. 3. Current density vs. mass fraction of water vapor at cathode surface based on free-convection mass transfer.

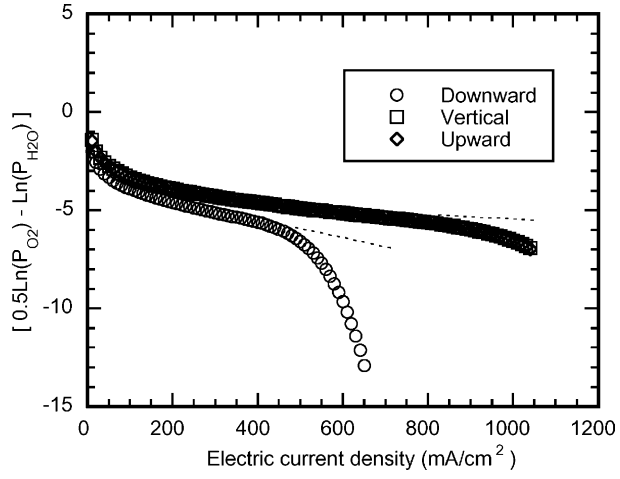

Fig. 5. Relationship of current density and the difference of the logarithm partial-pressures for oxygen and water vapor at the cathode surface.

V–I curve of a fuel cell. An excessive drop in $(\ln(P_{O_2}^{0.5}) - \ln(P_{H_2O}))$ can be found at a certain fuel cell current density. This can be viewed as a limitation of current density due to the weak mass transfer from using the free-convection mode.

In the above analysis, the existence of water vapor is ignored when the mass transfer of oxygen is reviewed, and vice versa when the water vapor is analyzed. This gives the optimum estimate of the mass-transfer coefficient and the maximum applicable current density by free-convection mass transfer. There is no doubt that a smaller maximum applicable current density below the estimated one will actually occur. Nevertheless, this analysis allows one to approximately estimate the capacity of the current density of a fuel cell if one selects the free-convection mode to supply oxygen.

3. Experimental results and discussion

Experimental work was performed using three types of PEM fuel cell units. The first two were purchased from Heliocentris Energy System Inc.: one is a stack of four fuel cells, and the other is a single-cell unit. The third fuel cell, which was designed by the authors and made in a laboratory, has a quite different structure from the commercial ones. The purchased cell stack and single-cell units' airside structures are illustrated in Fig. 6a, and the laboratory-made single-cell unit can be viewed in Fig. 6b. The purchased fuel cells were originally designed to use a forced airflow, while the new laboratory-made fuel cell is designed to use free-convection.

The two purchased fuel cells were installed with the air channels vertically oriented. A small fan could also be installed at top of the air channels to collect airflows from the channels in a suction mode. The voltage supplied to the small fan designates the airflow conditions of the fuel cell. For example, the nomenclature of A1 and A3 means that the voltages supplied to the small fan are 1 and 3 V, respectively.

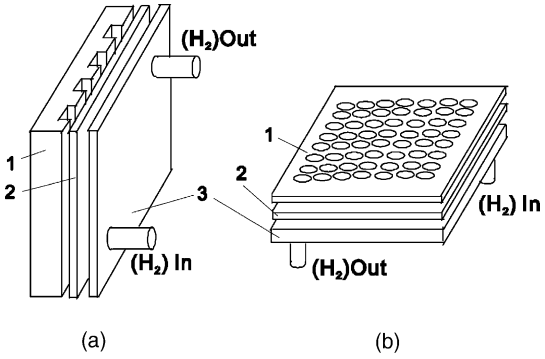

Fig. 6. Structure of air convection channel/surface (1: collector for air and cathode current, 2: electrode membrane assembly (EMA), 3: plate of anode collector with fuel channel). (a) The purchased cell stack and single-cell units' airside structures; (b) the laboratory-made single-cell unit.

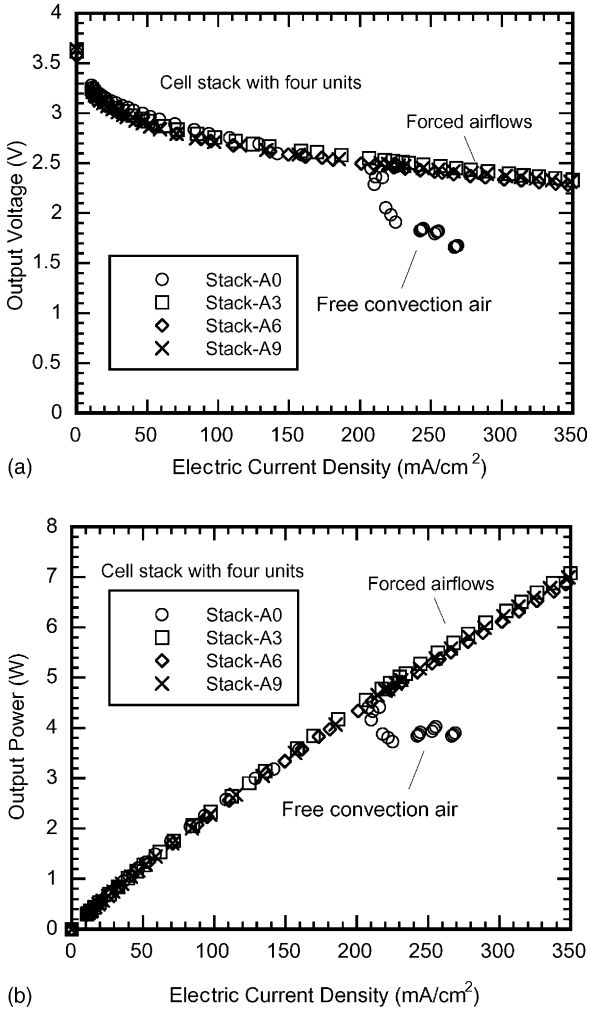

Fig. 7. Comparison of the cell stack performance between the different mass-transfer modes for oxygen. (a) Output voltage vs. current density, and (b) output power vs. current density for the cell stacks.

The free-convection case is represented by A0. The purchased cell stack and single-cell unit have active areas of 8.667 and 6.125 cm^2, for electrochemical reaction, respectively, while the laboratory-made single-cell unit has an active area of 0.3324 cm^2.

The output voltage and power versus the current density for the cell stacks are shown in Fig. 7a and b, known as the V–I and the P–I curves. In the low current density region, the free-convection mode can maintain the same performance as do by the forced convection mode. At high current densities, it is clear that forced convection airflow can feed oxygen while maintaining sufficiently high output voltages. For the free-convection mode, however, a dramatic drop in the output voltage occurs at a current density more than 200 mA/cm^2. Corresponding to this condition is a power output of 4 W from the cell stack. Qualitatively, this phenomenon agrees with the theoretical analysis conducted in the previous section.

In a similar manner, the purchased single fuel cell unit was tested and its electrical output versus the current density is

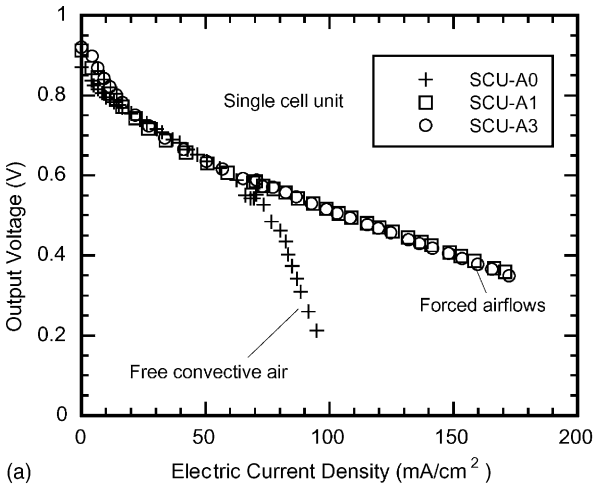

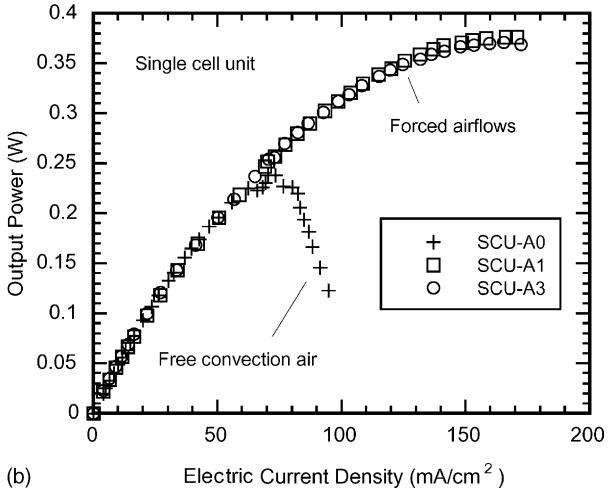

Fig. 8. Comparison of the single-cell performance between different mass-transfer modes for oxygen (SCU: single-cell unit). (a) Output voltage vs. current density, and (b) output power vs. current density for the purchased single fuel cell unit.

plotted in Fig. 8a and b. The same trend can be found that when the current density exceeds a certain value, the output voltage has an excessive drop for the free-convection case, while the case of forced airflow can still maintain a higher voltage. Because it depends on the different detailed structure and size of the fuel cell, the maximum current density available through the free-convection mode is relatively low in this case.

For the laboratory-made fuel cell unit illustrated in Fig. 6b, the free-convection air can reach the cathode surface through the mesh-like holes. As shown in Fig. 9, three orientations of the cathode surface (downward, vertical, and upward) were tested to find any differences in the fuel cell's performance. It was found that at a current density of around 185 mA/cm^2, the fuel cell reaches its maximum power, and after that the output power decreases dramatically. This is actually because of the significant drop of the output voltage of the fuel cell. Interestingly, the orientation of the cathode surface can result in a certain difference in output voltage.

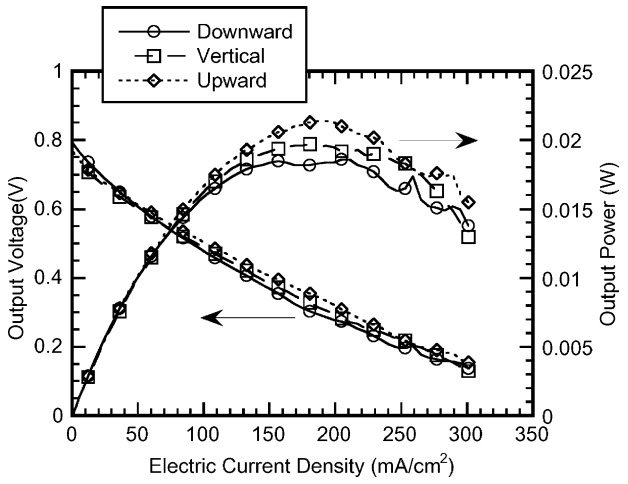

Fig. 9. Comparison of the single-cell performance at different orientations of the cathode plate.

Qualitatively, this phenomenon agrees with the conclusion of the theoretical analyses, although the difference of the output voltage is much less than in the analyzed results. The upward case has the best performance, while the downward orientation is not preferred because of its non-satisfactory performance. Through proper arrangement of the cathode surface, a current density of 200 mA/cm^2 might be maintained by adopting the free-convection mass-transfer mode to feed oxygen to the cathode surface.

4. Concluding remarks

The analogous phenomenon of free-convection heat and mass transport allows us to analyze the feasibility and the restrictions when a free-convection mass-transfer mode is utilized to feed oxygen to a PEM fuel cell.

It was shown in the theoretical analysis that the free-convection mass-transfer coefficient strongly depends on the difference in concentration of oxygen at the cathode surface and in the quiescent air. This is the reason that the mass-transfer rate strongly depends on the oxygen concentration at the cathode surface. We may view this in terms of the relationship of the fuel cell current density and the fuel cell voltage. Therefore, an investigation was conducted to see the applicable maximum fuel cell current density which the free-convection mass-transfer mode can sustain. Three important conclusions may be drawn from the study.

The theoretical analysis has derived expressions to obtain the maximum applicable current density for a fuel cell based on a free-convection mode at the cathode side; beyond the maximum point, an excessive drop of output voltage can occur, and output power is thus excessively reduced. Experimental testing has verified the existence of such a drop when the free-convection mode is adopted for PEM fuel cells.

However, at low levels of current density, a PEM fuel cell utilizing the free-convection mass-transfer mode does not

show any significant difference in its performance compared to a fuel cell using a forced air convection mode. Therefore, under such circumstances, free-convection mass transfer of air can be a very good choice for PEM fuel cells. A current density of up to 200 mA/cm^2 was experimentally operated for a commercial PEM cell stack and a laboratory-manufactured PEM fuel cell based on free-convection mode, which did not show any deterioration of output voltage compared to that operated in forced convection mode.

Orientation of the cathode surface can result certain differences in the performance of a PEM fuel cell. Due to its good performance, an upward orientation of the mass-transfer surface is preferred from our study. The maximum output power may be reduced by over 10% if one selects a downward orientation.

References

[1] S. Srinivasan, R. Mosdale, P. Stevens, C. Yang, Fuel cells: reaching the era of clean and efficient power generation in the twenty-first century, Annu. Rev. Energy Environ. 24 (1999) 281–328.

[2] C. Yang, P. Costamagna, S. Srinivasan, J. Benziger, A.B. Bocarsly, Approaches and technical challenges to high temperature operation of proton change membrane fuel cells, J. Power Sources 103 (2001) 1–9.

[3] T. Susai, A. Kawakami, A. Hamada, Y. Miyake, Y. Azegami, Development of a 1 kW polymer electrolyte fuel cell power source, J. Power Sources 92 (2001) 131–138.

[4] C. Wallmark, P. Alvfors, Design of stationary PEFC system configurations to meet heat and power demands, J. Power Sources 106 (2002) 83–92.

[5] G. Maggio, V. Recupero, L. Pino, Modeling polymer electrolyte fuel cells: an innovative approach, J. Power Sources 101 (2001) 275–286.

[6] A.A. Kulikovsky, Numerical simulation of a new operational regime for a polymer electrolyte fuel cell, Electrochem. Commun. 3 (2001) 460–466.

[7] E.R.G. Eckert, R.M. Drake, Analysis of Heat and Mass Transfer, McGraw-Hill, New York, 1972.

[8] F.P. Incropera, D.P. DeWitt, Introduction to Heat Transfer, 4th ed., Wiley, New York, 2002.

[9] Y.A. Cengel, M.A. Boles, Thermodynamics: An Engineering Approach, 2nd ed., McGraw-Hill, New York, 1994.

[10] I.M. Hsing, P. Futerko, Two-dimensional simulation of water transport in polymer electrolyte fuel cells, Chem. Eng. Sci. 55 (2000) 4209–4218.

[11] R.F. Mann, J.C. Amphlett, M.A.I. Hooper, H.M. Jensen, B.A. Peppley, P.R. Roberge, Development and application of a generalized steady-state electrochemical model for a PEM fuel cell, J. Power Sources 86 (2000) 173–180.

[12] T.E. Springer, T.A. Zawadzinski, S. Gottesfeld, Polymer electrolyte fuel cell model, J. Electrochem. Soc. 138 (8) (1991) 2334–2342.